JOURNAL OF MATERIAL SCIENCES 13 (1978) 415–420

Fracture mirrors in Columbia Resin CR-39

N. SHINKAI, H. SAKATA
Research Laboratory, Asahi Glass Co. Ltd., Yokohama 221, Japan

The relationship of fracture stress to mirror size for Columbia Resin, CR-39, is investigated. The fracture mirror constant is influenced by strain rate and test temperature, and gives values of 3.28 and 2.87 MN $m^{-3/2}$ for static and impact tests at room temperature, and 1.36 MN $m^{-3/2}$ for static tests at −150° C. The fracture surface energy for the initiation of unstable fracture decreases at high loading rate and at low temperature. Fractographic observations made on the fracture surface show some characteristic features reflecting the microstructure of this thermosetting plastic. The changes in the mirror constant and the fracture surface energy are discussed from the viewpoint of fracture mechanics.

1. Introduction

Fracture mirrors have generally been observed in the fracture surface of brittle materials such as inorganic glasses [1–3], polycrystalline ceramics [4, 5] and glassy polymers [6, 7]. In particular, for inorganic glasses and polycrystalline ceramics, an empirical relation has been found which gives a fracture mirror constant proportional to the fracture stress and the reciprocal of the square root of the mirror radius. Recently, this relation has been used successfully to predict the fracture surface energy and the fracture initiating flaw size based on fracture mechanics analysis [8, 9]. The fracture mirror constant for silicate glasses depends mainly on the chemical composition of the glasses and also on temperature conditions in the test [10, 11]. The fracture stress–mirror size relationship for glassy polymers, of which mechanical properties are strongly affected by strain rate and ambient temperature, is not yet well established.

The purpose of the present study is to investigate the effect of loading rate and test temperature upon the fracture mirror constant, the fracture surface energy and fracture morphology of glassy polymers. We chose a thermosetting resin, CR-39, as a test material, which is chemically termed allyl diglycol carbonate, because the fracture behaviour of thermosetting plastics is considered to be simple as compared with other well-known thermoplastics [7].

The brittleness of CR-39 makes it possible to introduce a controlled surface flaw-initiating fracture and to make a fracture mechanical analysis of the flaw.

2. Experimental procedure

The investigation was performed by using a commercial grade CR-39 sheet*. The cast-polymerized sheet is as transparent as plate glass. The test specimens were cut from the sheet into laths, 50 mm × 20 mm × 3 mm and 50 mm × 10 mm × 9 mm for static and impact tests, respectively. A definite minute flaw was introduced to initiate fracture at the centre of each specimen by pressing with a diamond indenter, 10 μm in radius, bearing a load of 100 g.

The fracture strength was determined in 3-point loading with support rollers 40 mm apart by use of an Instron type universal testing machine at crosshead speeds of 0.5, 1.0, 5.0 and 50 mm min^{-1}. In low temperature tests (−150° C) the specimens were placed in a chamber kept at that temperature by the method of jetting with liquid nitrogen.

The impact strength was measured at room temperature in 3-point bending over a span 40 mm using instrumented Charpy impact tester† which

*"Homalite 911" (SGL Industries, Inc., USA).

†"PSWO 30" from Shopper Corp., DDR.

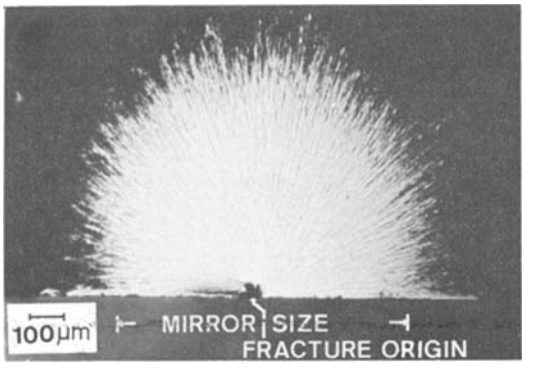

Figure 1 Fracture mirror of CR-39 broken in flexure at room temperature.

can record a load–deflection curve. The velocity of the hammer at impact was 5.6 m sec^{-1}.

The fracture surfaces were examined by optical and scanning electron microscope. The mirror size were measured by a 50-power optical microscope with ocular micrometer. The mirror radius was determined by measuring the distance between onsets of the mirror boundary on either side of the fracture surface edge and dividing by two (Fig. 1).

3. Results and discussion

3.1. Fracture stress versus mirror size

Variations of mirror size with fracture stress at room temperature and at −150° C are given in Fig. 2. Logarithmic plots of experimental data fit a straight line representing the following equation:

$$\sigma = A \cdot R_m^{-1/2} \qquad (1)$$

where σ is fracture stress, A, the so-called mirror constant, and R_m, mirror radius. The relationship between fracture stress and mirror size obtained at room temperature is very different from that at −150° C. The fracture test results for specimens with a definite flaw are summarized in Table I. The difference between the fracture mirror constants for static and impact tests at room temperature is rather small, although the mirror constant depends partially on the loading rate. Comparison of the mirror constant for room temperature tests and tests at −150° C shows a marked decrease in the mirror constant at low temperatures. Both the bending strength and Young's modulus increase at −150° C.

The fracture mirror constant corresponds to the particular stress intensity factor at the edge of the fracture surface roughness associated with micro-crack branching. The following equation for crack length at the crack branching for plane stress condition was proposed by Congleton and Petch [12]:

$$\sigma \cdot R_m^{1/2} = 2(E \cdot \gamma_m/\pi)^{1/2}, \qquad (2)$$

where R_m is the mirror radius substituted for the crack length at branching, E is Young's modulus, and γ_m the effective fracture surface energy for crack propagation. Although γ_m cannot be determined quantitatively from the mirror constant alone owing to the uncertainty in the appropriate Young's modulus during crack propagation, a decrease in the fracture mirror constant at −150° C indicates a decrease in the effective fracture surface energy in the dynamic state. This is due to an increase in Young's modulus as measured by the deflection of a beam (Table I). This trend is also supported by morphological changes in the appearance of fracture surfaces described in Section 3.2. Therefore, it can be considered that the decrease in plastic deformation

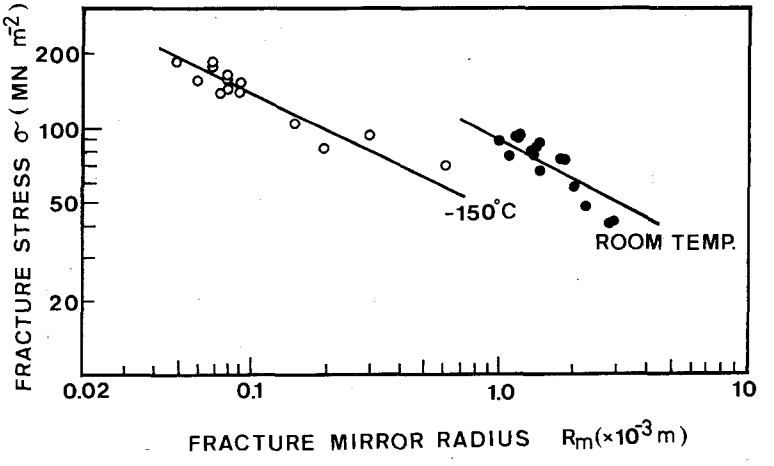

Figure 2 Relations between fracture stress and mirror radius of CR-39 at room temperature and at −150° C. (Solid lines show the equation: $\sigma \cdot R_m^{1/2}$ = constant.)

TABLE I Results of fracture tests for CR-39*

Test condition	Fracture stress σ (MN m^{-2})	Mirror radius R_m ($\times 10^{-3}$ m)	Mirror constant A (MN m$^{-3/2}$)	Young's modulus† E ($\times 10^3$ MN m^{-2})
Static bending (room temperature)	89.9 ± 5.0	1.33 ± 0.13	3.28 ± 0.25	2.16
Impact bending (room temperature)	117 ± 1.6	0.60 ± 0.04	2.87 ± 0.09	2.74
Static bending (−150° C)	152 ± 7.5	0.08 ± 0.01	1.36 ± 0.10	6.08

*These values are the average of 5 to 10 specimens with a definite surface flaw. Uncertainties are the standard deviation for each determination.
†Calculated values from the deflection of a beam specimen loaded at the centre.

that accompanies crack propagation at −150° C causes a decrease in fracture mirror constant. The effective fracture surface energy at room temperature decreases slightly with loading rate, since the crack propagates at a very high speed at the mirror boundary, regardless of static or impact loading conditions.

3.2. Morphology of fracture surface

A typical fracture pattern of CR-39 broken in bending is shown in Fig. 1. The fracture surfaces are characterized by three distinct regions; mirror surface, mist, and hackled areas. Macroscopically, these regions are similar to those observed on silicate glasses. However, microscopic examinations revealed some characteristic fracture features of CR-39.

First, the stable crack-growth region was observed in the fracture surface broken statically at room temperature, as illustrated in Fig. 3. The depth of this elliptical crack-growth region decreases as loading rate increases, and is rarely detected in the fracture surfaces produced by impact at room temperature and static bending at −150° C. Long narrow lines are noticeable in the mirror portion running radially from the initiation point to the mirror boundary. Sudden changes of direction of these lines at the boundary of the stable crack-growth region indicate a transition of fracture phase. These lines are thought to result from crack growing at slightly different planes.

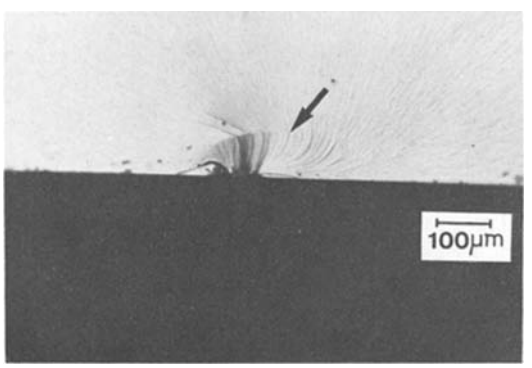

Figure 3 Stable crack-growth region in a fracture surface of CR-39, broken statically at room temperature. The arrow indicates a boundary of the region.

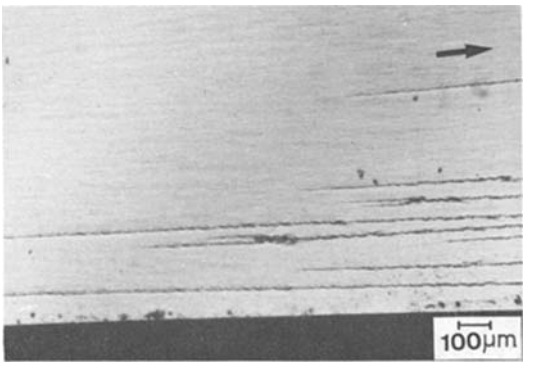

Figure 4 Radial river marks at mirror boundary. The arrow indicates direction of crack propagation.

Secondary cracks at the mirror boundary are radial river lines and appear abruptly as shown in Fig. 4. Scanning electron micrographs show that micro-crack branching occurs near the initiation of the secondary fracture, where some pore-like sources are observed, and flake patterns are conspicuous (Fig. 5). These morphological features are somewhat different from the mist zone of the mirror boundary of silicate glass and from the parabolas on the fracture surface of polymethylmethacrylate (PMMA). Considering that similar

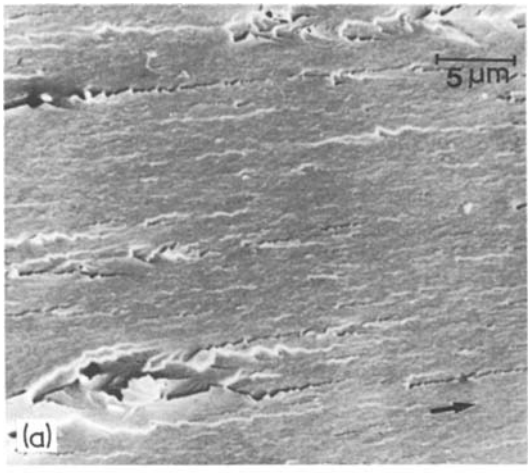

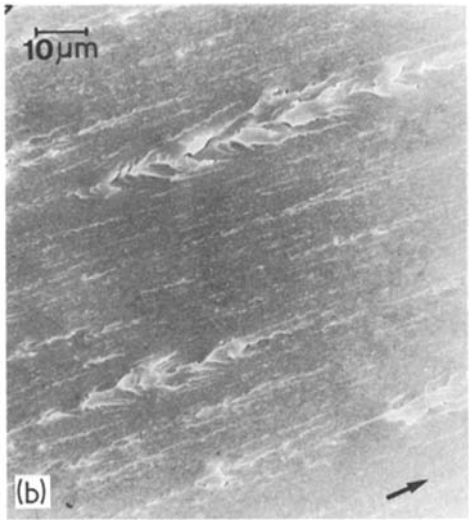

Figure 5 Scanning electron micrographs of micro-crack branching in boundary region of CR-39 fractured at room temperature. (a) Initiations of radial river marks, (b) Flake patterns at boundary region. The arrow indicates direction of crack propagation.

characteristics have been found on fracture surfaces of thermosetting resins, e.g., epoxy, polyester and phenolformaldehyde [13–15], it can be said that these characteristics arise from the highly cross-linked structures of thermosetting plastics.

Fig. 6 shows a change in the appearance of the fracture mirror produced at −150° C. It is interesting to note that the boundary region is broader and becomes more roughened than that at room temperature, and the ratio of the mirror radius to the initial flaw size is extremely small, as given in Table II. It has been shown that the mirror-to-flaw size ratio varies from material to material; the most polycrystalline ceramics show

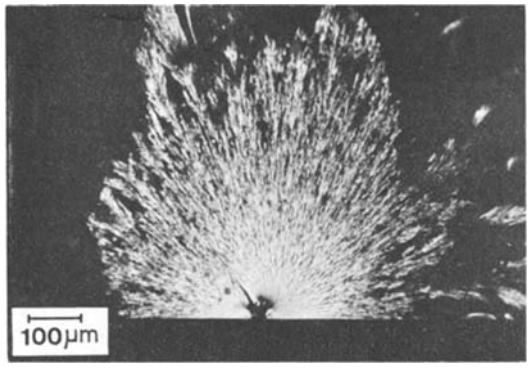

Figure 6 Fracture mirror of CR-39 broken in bending at −150° C.

smaller values and a broader boundary region than silicate glasses. These differences have been explained by the fracture process relating to the microstructural homogeneity and discontinuity [5, 16]. In comparing Fig. 5b with Fig. 7, the mirror boundary region produced at −150° C gives some evidence of a decrease in the amount of plastic deformation. The increase in roughness and width of the mirror boundary can be explained by the fact that CR-39 becomes brittle with a decrease in temperature, and this increases the opportunities for micro-crack branching, due to pores in CR-39, to occur. It can be concluded that the mirror constant depends on the microstructural continuity of CR-39 and on the fracture behaviour, which varies with the test conditions.

3.3. Fracture surface energy

Fig. 8 shows the changes in the fracture stress with loading rate at room temperature and at −150° C.

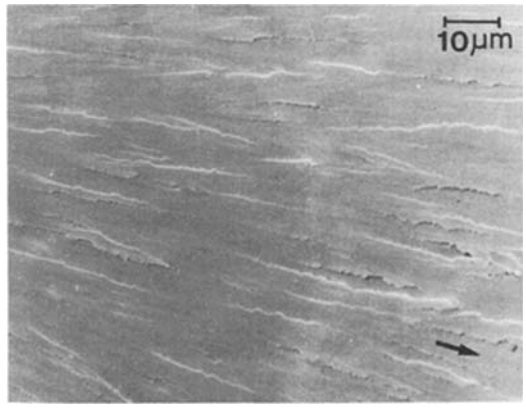

Figure 7 A mirror boundary region of CR-39 fractured at −150° C. The arrow indicates direction of crack propagation.

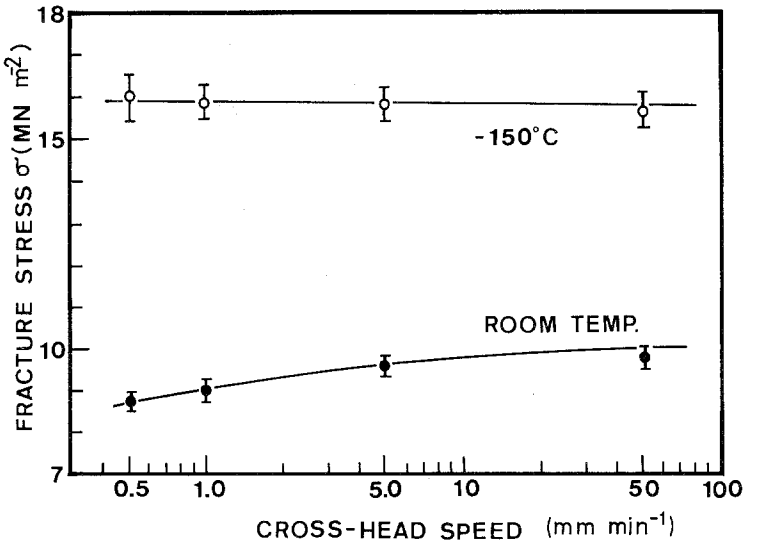

Figure 8 Dependance of fracture stress on loading rate for CR-39 at room temperature and at −150° C.

Fracture always originated from the definite flaw artificially made by indentation. The scattering in the measured strength was quite small; about 5% of the average value. The fracture stress at room temperature increases with increasing loading rate. At −150° C the change of fracture stress with loading rate is hardly noticeable. This small change in the strength means that subcritical crack growth hardly occurs in the initial stage of fracture at −150° C. For impact tests at room temperature, it can also be expected that the initial flaw will only have to enlarge slightly before reaching a critical size.

On the basis of a fracture mechanical analysis, the specific fracture surface energy, γ_c, for unstable fracture can be predicted from the ratio of the fracture initiating flaw size to the mirror radius, using the following equation [9];

$$\gamma_c = (a/R_m)(A^2/(Y^2E))^{1/2} \quad (3)$$

where a is critical size of initial flaw and $Y = (1/1.12)(\pi/2)^{1/2}$ for a penny-shaped surface crack.

Table II gives calculated values of γ_c from experimental data using Equation 3 on the assumption that the initial flaw is a penny-shaped crack. The critical flaw size for a specimen broken statically at room temperature was determined by measuring the size of the stable crack-growth region. To check these calculated values of γ_c, a separate measurement of γ_c was made using double-cantilever beam specimens (80 mm × 30 mm × 3 mm) at a displacement rate of 5.0 mm min^{-1}. The value of γ_c obtained at −150° C was 1.25×10^2 J m^{-2}, which agreed satisfactorily with that calculated value as given in Table II. However, γ_c at room temperature could not be determined exactly, because crack-arrest occurred. This crack-arrest phenomenon seems to be similar to that observed in epoxy resin, which has been explained as being due to localized plastic yielding at the crack tip, or the diffusion of reactive species such as water to the crack tip [13, 17]. Since a material which undergoes crack jumping is necessarily subjected to varying crack velocity, and γ_c varies with crack velocity, it is difficult to measure an exact value γ_c for an initiation of fracture or arrest parameter. Generally, crack stability depends on the geometry of the specimen and the loading mode. A specimen with a definite surface flaw, loaded in bending, can be used to estimate the specific fracture surface energy because crack arrest does not occur.

As presented in Table II, γ_c of CR-39 decreases at high loading rate and also at low temperature. The decrease in γ_c with a drop in temperature is

TABLE II The fracture surface energy for CR-39

Test condition	Fracture surface energy γ_c (J m^{-2})	Mirror-to-flaw-size ratio R_m/a
Static bending (room temperature)	260 ± 20	15.6
Impact bending (room temperature)	160 ± 5	15.0
Static bending (−150° C)	120 ± 10	2.0

the opposite behaviour to that of PMMA, which shows a marked increase in γ_c as the temperature is reduced [18]. In addition, no interference colours were detected in an observation of the fracture surfaces in CR-39 under reflected light. Since these colours are caused by crazing formed as a result of an orientation effect of polymers during fracture, this means that stress crazing as observed in PMMA rarely occurs in CR-39. The increase in γ_c of PMMA at low temperatures has been considered to indicate that the externally supplied energy required to form a craze layer must increase as segmental mobility decreases at low temperature. Therefore, the difference between the change in γ_c of CR-39 and that of PMMA may be attributable to the fact that thermosetting plastics are thermally cross-linked and are more brittle than thermoplastics. It can also be concluded that an increase in strain rate and a drop of temperature inhibit relaxation processes and hence decrease both critical flaw size and dimension of the fracture mirror in CR-39.

4. Conclusion

Fracture stress and mirror size of a thermosetting glassy polymer, CR-39, are measured and the relationship (fracture stress) $\times$ (mirror radius)$^{1/2}$ = constant, which has been established for silicate glasses and polycrystalline ceramics, is confirmed for this plastic.

The fracture mirror constant obtained at room temperature is about 3.28 MN m$^{-3/2}$, which is slightly affected by loading rate and is 2.4 times as great as that at -150° C. The specific fracture surface energy estimated from the mirror constant and fracture initiating flaw size decreases under impact loading and at low temperatures, which coincides with that obtained from double-cantilever beam measurements at low temperatures.

Morphological studies on fracture surfaces indicate that some characteristic features are due to the cross-linked structure of thermosetting resins, and that the formation of the mirror boundary depends mainly on the microstructural continuity of CR-39.

Acknowledgement

The authors thank Mr H. Ishikawa for his technical assistance in the scanning electron microscopy.

References

1. W. C. LEVENGOOD, *J. Appl. Phys.* **29** (1958) 820.
2. E. B. SHAND, *J. Amer. Ceram. Soc.* **42** (1959) 474.
3. J. W. JOHNSON and D. G. HOLLOWAY, *Phil. Mag.* **14** (1966) 731.
4. H. P. KIRCHNER and R. M. CRUVER, *ibid* **27** (1973) 1433.
5. J. J. MECHOLSKY, S. W. FREIMAN and R. W. RICE, *J. Mater. Sci.* **11** (1976) 1310.
6. I. J. LESUWERIK, *Rheologica Acta* **2** (1962) 10.
7. A. S. TETELMAN and A. J. McEVILEY, "Fracture of Structural Materials" (Wiley, New York, 1967) p. 621.
8. D. A. KROHN and D. P. HASSELMAN, *J. Amer. Ceram. Soc.* **54** (1971) 411.
9. J. J. MECHOLSKY, R. W. RICE and S. W. FREIMAN, *ibid* **57** (1974) 440.
10. N. SHINKAI, *Japan. J. Appl. Phys.* **14** (1975) 147.
11. N. J. KERPER and T. G. SCUDERI, *Amer. Ceram. Soc. Bull.* **43** (1964) 622.
12. J. CONGLETON and N. J. PETCH, *Phil. Mag.* **16** (1967) 749.
13. K. SELBY and L. E. MILLER, *J. Mater. Sci.* **10** (1976) 12.
14. A. CHRISTIANSEN and J. B. SHORTALL, *ibid* **11** (1976) 1113.
15. B. E. NELSON and D. T. TURNER, *J. Polymer Sci.* **B9** (1971) 677.
16. R. W. RICE, "Surface and Interfaces of Glass and Ceramics", edited by V. D. Frechette, W. C. Lacource and V. L. Burdick (Plenum Press, New York, 1974) p. 450.
17. R. J. YOUNG and P. W. R. BEAUMONT, *J. Mater. Sci.* **11** (1976) 776.
18. J. P. BERRY, *J. Polymer Sci.* **A1** (1963) 993.

Received 10 May and accepted 8 June 1977.